POLITECNICO
MILANO 1863

SCUOLA DI INGEGNERIA INDUSTRIALE
E DELL'INFORMAZIONE

von KARMAN INSTITUTE
FOR FLUID DYNAMICS

Executive Summary of the Thesis

Efficiency of a high-speed Low Pressure Turbine measured in an intermittent short-duration facility

Laurea Magistrale in Mechanical Engineering - Ingegneria Meccanica

Author: Davide Visconti

Advisor: Prof. Paolo gaetani

Co-advisor: Prof. Sergio Lavagnoli

Academic year: 2021-2022

1. Introduction

During the last decades, more stringent legislation and a stronger sensibilization about environmental issues pushed aviation industry to find new strategies to improve efficiency. On this purpose, Geared Turbofan aeroengines have been designed. The objective of this report is to determine the efficiency, with an accuracy better than 1%, of a High speed low pressure (HSLP) turbine stage. Such a low level of uncertainty requires the accurate evaluation of a large number of quantities simultaneously, as the mass flow rate of the mainstream, as well the one of secondary flows (purge and leakage), the inlet total pressure and temperature, stage exit total pressure, shaft power, mechanical losses and the heat transfer. This report summarizes the results obtained during a seven months short training program (STP) in the frame of the SPLEEN research project carried out at the Von Karman Institute for Fluid Dynamics in Belgium.

2. Generalities

2.1. Experimental Test Facility

The whole SPLEEN test campaign was conducted on the CT-3 test rig, capable of testing full scale turbine stator blade rows of advanced aircraft engines. It is able to simulate Mach number, Reynolds number, Turbulence intensity and Gas/wall/coolant temperature ratios in real modern aeroengine representative conditions and in a cost-effective way (compared to continuously running facilities).
Before running a test, with the turbine stage isolated from the upstream compression tube by a fast opening shutter valve, test section and dump tank are evacuated to $\sim 30\ mbar$ and the rotor turbine is spun up to 90-95% the design speed ($\sim 4500\ rpm$). The test start injecting cold high-pressure air to the back of the cylinder, which starts travelling forward compressing, quasi-isentropically, the air in the second chamber. When here, a target level of pressure and temperature are achieved, the shutter valve is opened and the hot compressed air flows through the turbine stage before being discharged in the dump tank. Reynolds number is controlled by triggering the shutter opening when inside the cylinder the right temperature and pressure levels are reached. Mach number and mass flow rate are instead regulated by a sonic throat placed between outlet turbine and dump tank. More details about the operation of the facility are reported by Sieverding and Arts (1992). As shown in Figure 1, after a short tran-

sient, nearly constant flow conditions are maintained for 0.3-0.4 s and, before the test end, a 100 ms common time-window for data averaging is selected for all the measurements.

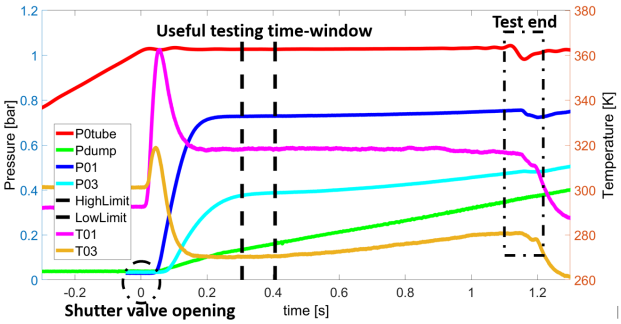

Figure 1: Time evolution of relevant quantities during the blow-down

2.2. HSLP Turbine Stage

The geometry of the flow-path is a one-to-one scale of the first stage of a HSLPT and consists of a stator and a rotor featuring 96 vanes and blades resulting in a pitch of 3.75° between each airfoil. Blade airfoils are turned and twisted (shrouded), specifically designed to recreate the aerodynamic behavior (in terms of exit speeds, loading and losses) and ensuring operating conditions of research interest: high Mach (> 0.7, at stator exit) and low Reynolds numbers ($< 10^6$). The stage has been designed to work with an expansion ratio $\beta = \frac{P_{03}}{P_{01}} = 0.527$, flow coefficient at rotor inlet $\phi = 0.6$, blade loading coefficient $\psi = 1.8$, reaction degree $\chi = 0.45$, stator inlet Reynolds number $Re_1 \sim 10^5$ and stage inlet mass flow rate of 10.57 kg/s. The tested LPT stage features a rotor assembly configuration that does not include labyrinth seals. In so doing, it is possible the injection, together with the mainstream, of purge flows coming from the stator-to-rotor hub cavities. During the test campaign, depending on the purge flow intensity, two operating conditions were tested: *Nominal mode* with purge flow rate equal to 0.5% of the mainstream one and *High mode*, with purge flow rate equal to 1% of the mainstream one. The downstream purge flow is set equal to zero. Efficiency measurements are mainly concentrated in four key regions: Plane 01 (74.04 mm upstream of the vane leading edge), Plane 03 (15.4 mm downstream of the blade trailing edge), Upstream and Downstream hub cavity.

3. Diabatic Efficiency Measurements

Unlike continuously running test rigs, the efficiency estimation in intermittent short duration facilities is quite challenging because of the very short time test duration of about 0.4 s and the non-adiabatic state. In order to measure the efficiency, the *Mechanical method* has been adopted, rather than the *Thermodynamic method*. In fact, although the latter allows computing the efficiency span-wisely, it requires very accurate measurements of the upstream and downstream total temperature and pressure along the span and the thermodynamic quantities at the stage outlet are quite challenging to characterize with high precision. The Mechanical method, instead, provides an integral value of the efficiency and it is based on the torque measurement of the turbine rotor:

$$\eta = \frac{P_{real}}{P_{ideal}} = \frac{T_{shaft}\omega + P_{losses}}{P_{ideal}} \qquad (1)$$

Due to the very small testing time, VKI CT-3 test rig operates under iso-thermal condition at the walls and therefore surface heat transfer occurs and the process, theoretically, can not be approximated as adiabatic. The entropy at turbine stage exit also depends on the heat transfer during the process and without a proper estimate of this quantity, the measured efficiency will be a function of the heat lost through all the stage. Although it is common practice to define efficiency for non-adiabatic expansion processes respect to an isentropic process, it is more logical to define it respect to a process with the same heat transfer as the real one, but with no irreversibilities that would give rise to additional entropy changes. That is, the reference process in non-isentropic but nonetheless reversible [3]. The isentropic efficiency, instead, is derived by considering an ideal expansion process that is both adiabatic and reversible. It considers only the losses, or entropy generation, due to aerodynamic phenomena. Here instead, also the heat transfer effects must be accounted for. The different processes mentioned so far are depicted in Figure 2.

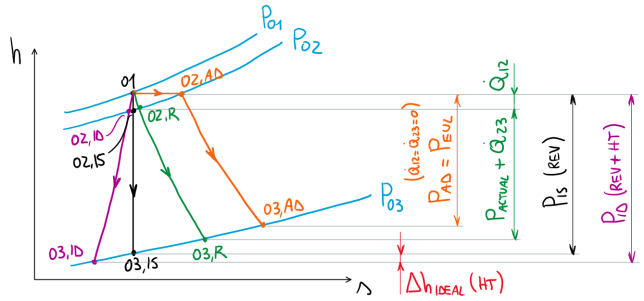

Figure 2: Thermodynamic diagram representation of the four possible expansion processes: Orange: Adiabatic expansion; Green: Diabatic expansion; Black: Isentropic expansion; Purple: Ideal expansion (non-isentropic but reversible)

Referring to Figure 2, the specific power from the ideal reference process may be derived as the combination of the specific power from the isentropic process and the change in exit enthalpy as result of the heat transfer during the expansion, $(\Delta h_{ideal}(HT))$ [3]. Therefore:

$$\eta_{diab} = \frac{h_{01} - h_{03,R}}{h_{01} - h_{3,ID}} = \frac{P_{actual} + \dot{Q}}{P_{is} + \Delta H_{ideal}(HT)} \quad (2)$$

The correction term is, formally, the integral of $\frac{\delta Q}{T}$, but it can be estimated by assuming that the heat transfer occurs at the mean temperature between the inlet and outlet of the stage [2]. Which yields the following expression:

$$\Delta H_{ideal} \sim T_{03,is}\left(\frac{\dot{Q}_{12}}{T_{01}} + \frac{2\dot{Q}_{23}}{T_{02} + T_{03,is}}\right) \quad (3)$$

Note that the evaluation of this correction term requires a detailed knowledge of the full temperature and heat transfer fields.
The isentropic power is evaluated according to:

$$P_{is} = \int_{01}^{03,is} dH = \int_{01}^{03,is} C_p dT \sim$$
$$\sim C_p \int_{01}^{03,is} dT = C_p T_{01}\left(1 - \beta^{\frac{\gamma-1}{\gamma}}\right) \quad (4)$$

C_p and γ air properties are evaluated at an average temperature between T01 and T03,is. As it will be shown in the uncertainty analysis, these two parameters have high *Sensitivity Coefficients* for the efficiency, hence, it is very important to determine them with a good accuracy.

3.1. Adiabatic and Diabatic Efficiency

The adiabatic process (real, without HT) and the isentropic expansion (reversible, without HT) are used to compute the adiabatic-isentropic efficiency, characteristic of continuously running facilities. The diabatic process (real, with HT) and the ideal expansion (non-isentropic but reversible, with HT) are, instead, used to estimate the diabatic efficiency, characteristic of transient rigs (CT-3).
N. Atkins and R. Ainsworth in [2] shows a simple technique to decouple the effects of heat transfer and aerodynamic irreversibility such that the results of turbine performance measurements under diabatic conditions can be compared with the ones obtained under adiabatic mode. This correction is sufficient to derive the adiabatic-isentropic efficiency from the diabatic efficiency results of engine representative non-adiabatic testing. Looking at Figure 2, the adiabatic-isentropic efficiency can be defined as:

$$\eta_{ad} = \frac{P_{actual} + \dot{Q}}{P_{is}} - \frac{H_{03,ad} - H_{03,r}}{P_{is}} \quad (5)$$

The second term of Equation 5 is the fraction of the total ideal enthalpy lost due to the total heat transfer taking place across the stage. The calculation of this term refers to the *"Exit enthalpy correction"*. This is an analogous problem to the one seen for the determination of the ideal process in Equation 2 and in fact, even in this case, the rigorous solution of the integral can be skipped and the *Exit enthalpy correction* can be approximated by Equation 3.
In the efficiency definitions, the expansion of the purge flow must be also considered, with the relative properties (C_p and γ).
Note that all the formulations presented so far, are valid for a streamline or if the stage profiles of total pressure and temperature are uniform along the respective inlet and exit planes of the control volume (Plane 01 and Plane 03). Unfortunately, although the inlet quantity distributions are quite regular along the span, these conditions are not satisfied, at all, at the outlet. It is crucial to use pressure and temperature values that characterize the whole flow condition and the mid-span quantities

alone do not represent entirely the flow field. For this reason, in the efficiency equations, *Mass flow averaged* quantities along the span will be used, computed according to:

$$\tilde{X} = \frac{\int_{Rhub}^{Rtip} X \rho V 2\pi r \, dr}{\int_{Rhub}^{Rtip} \rho V 2\pi r \, dr} \tag{6}$$

4. Uncertainty Analysis

Is has been conducted, according to ASME specifications [1], on each term involved in the efficiency formulation, as well as, on the final performance parameter itself. In engineering field, any experimentally measured value has an inherent error associated with it which leads to an uncertainty in the derived result. The total error is commonly expressed as combination of: *Random precision error* and *Systematic bias error*. The first one defines the repeatability of a measurement, it determines the smallest change in efficiency that can be resolved and it changes test by test. The second component, instead, is an offset, it does not change but it remains constant during all the tests. In order to combine together all the uncertainties associated to each single quantity involved in the efficiency definitions, the *Root Sum Square (RSS)* is used:

$$\Delta\eta = \sqrt{\sum_{i=1}^{N} \left(\frac{\partial \eta}{\partial x_i} \Delta x_i \right)^2} \sim \sqrt{\sum_{i=1}^{N} {\Delta\eta_i}^2} \tag{7}$$

In Equation 7, $\frac{\partial \eta}{\partial x_i}$ terms are the *Sensitivity Coefficients*. The efficiency error can be computed both solving the exact partial derivatives or, if they are too complex to be expanded in Taylor series, the approximation shown in Equation 7 can be adopted $\left(\frac{\partial \eta}{\partial x_i} \sim \frac{\Delta \eta}{\Delta x_i} \right)$. It is standard to quote the total uncertainty of a variable X to a 95% Confidence level.

5. Heat Transfer Estimation

During the WP2 SPLEEN test campaign, any heat transfer measurements were taken. This is because, being a LP turbine, the overall heat flux is expected to be very small. In fact, the temperatures that are reached inside the test section are modest, if compared with the ones achieved, for example, in a HP turbines. For this reason, it is pointless investing in heat transfer measurements. However, an estimate of the overall amount of heat through the wall stage must be provided to confirm this hypothesis and to compute the final efficiency.
The control volume adopted for the computation is the same of the efficiency estimation: Volume comprised between Plane 1 and Plane 3. The overall control surface has been sub-divided in different parts according to Figure 3 and the heat transfer has been estimated through each of the five sub-sections: Stator and rotor blade surfaces, Tip and hub stator and rotor endwalls and the annulus channel upstream the vanes.

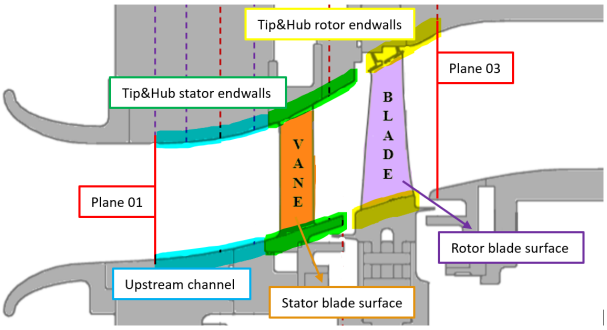

Figure 3: Meridional view of the test section highlighting the control surface subdivision

In the heat flux estimation, just the convection mode is considered, neglecting both conduction and radiation. The convective heat transfer, between gas and stage walls, is expressed by the Newton law:

$$\dot{Q}_{conv} = hS \left(T_{hotgas} - T_{coldwalls} \right) \tag{8}$$

Temperatures are known from measurements, the wetted surface S, for each sub-section, is estimated relying on CAD models of the stage, while the convective heat transfer coefficient h is evaluated exploiting *Nusselt* and *Stanton* number correlations. On this purpose, an *"hybrid approach"* has been employed to estimate the Nu and/or St number characteristic of each sub-section. In particular, both analytical correlations and numerical or experimental results are considered. Different papers, about heat transfer measurements on HP turbines, have been consulted and results adequately scaled based on Reynolds and Mach number characteristic of our problem. Firstly, the heat flux through the statoric components is computed.

In so doing, the relative total temperature at the rotoric components inlet, can be estimated as a function o the heat transfer through the surfaces between Plane 1 and Plane 2 (Equation 9).

$$T_{02,rel} = T_{01} - \frac{\dot{Q}_{tot,stator}}{\dot{m}_{main} C_{p,stator}} + \frac{W_2^2 - V_2^2}{2C_{p,2}} \quad (9)$$

At this point, also the heat lost in the rotoric components can be estimated. Correlations and methodology are the same of the stator, the only difference is the frame of reference (for the stator was absolute, for the rotor is relative).

Table 1: Overall heat transfer results

Quantity	Nominal value
Stator blades	1586.69 W
Stator endwalls	839.92 W
Upstream stator channel	1315.63 W
Overall Stator	3742.24 W
Rotor blades	-20.40 W
Rotor endwalls	-5.66 W
Overall Rotor	-26.06 W
Overall	3716.17 W

Experimental test-averaged results are summarized in Table 1. Note that the relative inlet total temperature to the rotoric components ($T_{02,rel}$) is so small that it is even lower than the walls temperature (negative values).
A parametric analysis has also been performed in order to get how heat transfer results change, as a consequence of a perturbation on the boundary conditions in the Newton equation. In particular, a perturbation of the cold walls temperature, stage inlet total temperature and equivalent Nusselt number has been accounted for. This brief study will be very useful in the final evaluation of the heat transfer impact on the efficiency.
Finally, an uncertainty analysis on the heat transfer through each single sub-section and on $T_{02,rel}$, has been performed. The two error components associated to each term that appears in the Newton equation has been estimated and then, by exploiting the RSS method reported in Equation 7, the final heat flux uncertainty is computed. In particular, the experimental test-averaged overall heat transfer is 3716.17 W, the random error component at 95% CL is $\sim$ 2% and the bias is 12.5%. The test-to-test repeatability amounts to 2.5%

6. Mass Flow Measurements

Due to the reduced size of the Laboratory, the mass flow rate across the stage cannot be measured in a *"Direct"* way by means of a *Venturi* or an *Orifice plate*. In fact, such systems, according to Standards, would require very long and straight tubes upstream and downstream the section in order to fully stabilize the incoming flow. For this reason, an *"Indirect" method*, based on a zero-dimensional model of the facility developed by L. Porreca and R. Dénos [5], has been adopted. It simply consists in monitoring the mass of air inside the tube as a function of time (Equation 10). Indeed, the pressure and the temperature of the gas can be measured and, once the piston position and displacement are known (x), the volume of the air is also known, as well its mass.

$$\dot{m}_{tube} = \frac{\mathrm{d}m_{tube}}{\mathrm{d}t} = \frac{P_{0,tube}}{RT_{0,tube}} \frac{\pi D_{tube}^2}{4} \frac{\mathrm{d}x}{\mathrm{d}t} \quad (10)$$

In order to have a coherent estimate of all the quantities that appears in Equation 10, the zero-dimensional model is used to fit the measured traces of different signals. The model performs mass and energy balances as a function of time in different volumes of the facility (i.e. two volumes inside the cylinder, settling chamber and dump tank). The model accounts also for the secondary flows, however, just the purge flow is considered, while the leakage (in both the two hub cavities) is neglected.

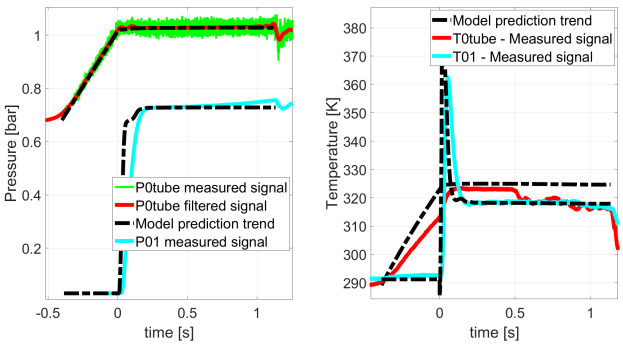

Figure 4: Matching between experimental measurements and model prediction of total pressure and temperature inside the tube and at the stage inlet

In Figure 4, an example of match between measured signal and thermodynamic quantities evolution foreseen by the model is shown. It is possible to see a delay in the P_{01} signal due to a small difference in the volumes considered by the model, with respect to those of the real plant. Moreover, also the total temperature inside the tube is bad-matched. This is because the temperature measurements inside the cylinder are quite challenging due to the probe position (the circulation of the flow is not optimum) and to the bad response of the thermocouple. Anyway, what is interesting is just the match in correspondence of the useful testing time-window.
A key point of the correct operating condition of such facility is that during a test, any mass accumulation or loss must occur. To do that, once the sonic throat downstream the turbine stage has been regulated to set the wanted mass flow through the test section, a valve, upstream the cylinder, must be properly opened to ensure the conservation of the mass flow in all the sections of the facility. Namely, what is exiting from the tube must be equal to what is discharging in the dump tank. With a perfect regulation, the pressure trace remains flat. In order to account for possible differences between the tube exit and the stage inlet (separated by a settling chamber), the turbine is assimilated to a sonic orifice and the mass flow can be computed with the well-known equation:

$$\dot{m}_{01} = \frac{P_{01}}{\sqrt{T_{01}}} A_{eff,stage} \sqrt{\frac{\gamma}{R}\left(\frac{2}{\gamma-1}\right)^{\frac{\gamma+1}{\gamma-1}}} \qquad (11)$$

In Equation 11, P_{01} and T_{01} can be measured, while, in order to determine the $A_{eff,stage}$, an *"Artificial test"* is run with the "best tests". The test is run for each operating condition so that, during the blow-down, the total pressure inside the tube is perfectly constant. Under this condition, the mass flow conservation is verified among each single section of the facility and the $A_{eff,stage}$ computation is now straightforward.
For the nominal operating condition, the stage inlet mass flow results in 10.62 kg/s, while for the high mode it is equal to 10.66%. The repeatability is 0.18% and 0.15% respectively for nominal and high purge condition.
A Sensitivity analysis, together with a study about the influence, on the inlet stage mass flow rate, of the parameters governing the zero-dimensional model, have been performed. This allows to understand which are those quantities that mainly influence the mass flow and that are considered in the Uncertainty analysis. For the nominal purge, the random error is 0.27% and the bias 0.93%, while for the high purge, the random is 0.41% and the bias 0.94%.

6.1. Secondary flows

The Mass flow rate of purge is measured during the injection inside the upstream hub cavity by means of an orifice which is always chocked, relying on the relation already presented in Equation 11. It is sufficient measuring the total temperature and pressure upstream the throat and the diameter of the orifice. On average, the purge flow is 0.054 kg/s ($\sim$ 0.5% of the mainstream one) and 0.107 kg/s ($\sim$ 1% of the mainstream one), respectively, for nominal and high purge mode.
The leakage mass flow rate is found monitoring pressure (P_0) and temperature (T_0) inside the upstream hub cavity, known the volume (V) from CAD models, by means of:

$$\dot{m}_{leak} = \frac{V}{R}\left(\frac{1}{T_0}\frac{\mathrm{d}P_0}{\mathrm{d}t} - \frac{P_0}{T_0^2}\frac{\mathrm{d}T_0}{\mathrm{d}t}\right) \qquad (12)$$

The leakage mass flow has been evaluated considering zero, nominal and high purge. Anyway, independently on the operating condition, it results to be always lower than 0.001 kg/s, that means, two order of magnitude lower that the systematic uncertainty of the mainstream mass flow rate ($\sim$ 1%) and for this, totally negligible.
A parametric analysis has also been performed in order to account for possible measurements inaccuracy and probes non-reliability. In any case, the leakage mass flow remains still lower than 0.001 kg/s although the imposed variation of 20% of the thermodynamic quantities inside the volume.

7. Rotational Speed, Acceleration and Inertia

The actual aerodynamic power produced by the turbine is given by the product between the rotational speed of the rotor and the tangential forces that develop in correspondence of each

blade as a consequence of the pressure difference, created by the airfoil profile, between the pressure side and the suction side. However, this quantity cannot be directly measured and the solution is to monitor the torque generated by the turbine shaft. Since CT-3 test facility is not supplied with an aero-brake, during each test, the rotor turbine is free to accelerate. By measuring this acceleration, together with the rotational speed and the rotor inertia, it is possible to characterize the mechanical power developed by the turbine, according to Equation 13. Note that some parasitic losses need to be quantified since the power measured at the shaft is slightly lower than the aerodynamic one produced at blades level. In fact, some mechanical energy is dissipated in the bearings and by the disc windage losses.

$$P_{aero} = J\omega\dot{\omega} + (T_{bearings} + T_{windage})\,\omega \quad (13)$$

In order to quantify the power losses, acceleration-deceleration tests with the facility open, should be conducted. However, since it was not possible to do that, a correlation proposed by R. Dénos et al. [4] has been employed.

7.1. Inertia measurement

The methodology which is followed for the inertia measurements is the one proposed by Haldeman and Dunn, 1996. The method consists in performing both an acceleration and deceleration of the rotor disc, during the same test, using a known torque which is generated by leaving a weight falling down.

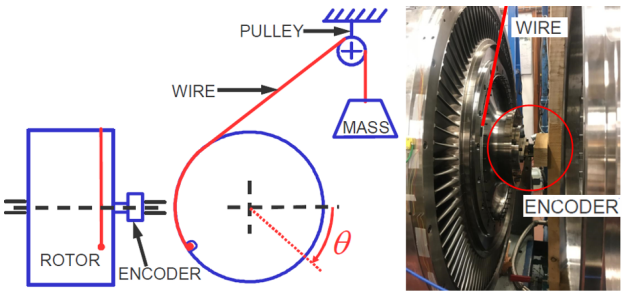

Figure 5: VKI experimental setup

In Figure 5, the whole experimental setup is depicted. The rotor assembly is connected to the hang mass with a plastic coated steel wire, by means of a pulley connected to the ceiling. The angular displacement of the rotor is monitored by a digital encoder (1024 pulses per revolution) sampled at 1 MHz with a digital counter. The overall test is divided in two phases:

1. **Phase 1 - Acceleration**: between ta and tb, the mass is falling down accelerating the rotor. The rotor velocity increases linearly, while the angular displacement follows a quasi-perfect parabolic law, as shown in Figure 6.

$$\Delta E_{potential} = \Delta E_{kinetic} + \Delta E_{friction} \quad (14)$$

2. **Phase 2 - Deceleration**: between tc and td. The mass touches the ground (peak in the velocity or concavity change in the angular displacement plot, Figure 6), the weight stops pulling the rotor and it starts decelerating by friction.

$$0 = \Delta E_{kinetic} + \Delta E_{friction} \quad (15)$$

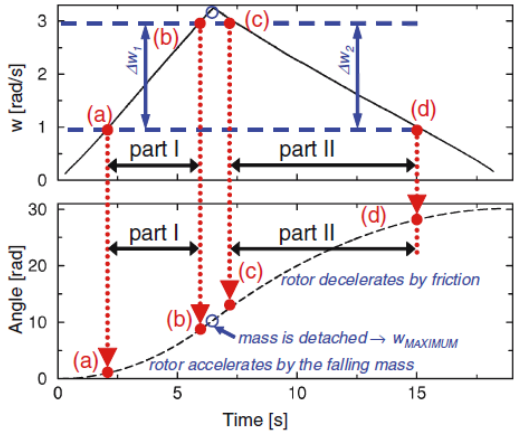

Figure 6: Linear velocity and parabolic angular displacement of the rotor

Depending on how the friction term is modelled, different methodologies can be adopted. In the current study it was decided, initially, to model this term as a constant [7], independently on the rotational speed and then, it was assumed a linear function of the velocity [6]. In the last two mentioned papers, all the equations used in this study are collected and, for the sake of brevity, are not reported here. Anyway, by combining the two equation of motions written during the acceleration and deceleration phase, it is possible to compute the inertia of the rotor,

by solving a linear system (in the first case) and by performing a multi-dimensional optimization in the second case (more complex and time-consuming).
Unfortunately, at the end of the experimental tests, the value of the inertia was not satisfactory at all. For this reason, the efficiency estimation has been carried out with the value estimated with CAD models: 13.496 kgm^2 with an error of 0.45%.

8. Efficiency results

Efficiencies were computed for each test and averaged to produce the results given in Table 2. The dispersion reported refers to a single experiment and results from the standard deviation of 16 tests, for the nominal, and 12 for the high purge condition.

Table 2: Average results for the four efficiency definitions

	Nominal purge		High purge	
Definition	**Mean Eff**	**STD (95%)**	**Mean Eff**	**STD (95%)**
Diab Indicated	0.9233	0.79%	0.9164	0.98%
Diab Mechanical	0.9166	0.86%	0.9100	1.02%
Thermodynamic	0.9091	2.62%	0.9184	1.88%
Adiabatic	0.9228	0.80%	0.9159	0.99%

The dispersion is a bit disappointing (compared to the results obtained in previous test campaigns), but this is mainly due to the expansion ratio (PDC). Namely, difficult measurements of pressure on Plane 3 (the pressure probe had a very slow response). Unfortunately this term has a very high sensitivity ($\sim$ 1.5). Note, especially, the high dispersion associated to the thermodynamic efficiency. This is expected, as anticipated initially. Anyway, the final results confirm a high level of efficiency which can be expected since the stage was designed at the state of the art. This range is also confirmed by a brief comparison with other experimental turbines on the *Smith chart*. The heat transfer impacts for a 0.67% and 0.65%, respectively for nominal and high purge, on the efficiency. Moreover, a reduction of 0.7% of the efficiency is experienced for an increase of the purge flow of 100% (it doubles), passing from 0.5% to 1% of the mainstream mass flow rate.
Both systematic (bias) and random error component have been computed starting from the uncertainties of each single quantity that appears in the efficiency formulations seen so far. The uncertainty analysis has been conducted on all the 4 efficiency definitions and for each operating mode. There are some terms that have just one error component, i.e. Inertia and Power losses (Plosses) do not have the random error, but just the systematic one. On the other hand, the thermo-physical properties of the working fluid (γ and C_p), the rotor rotational speed and acceleration, do not have any bias error component but just the random one. All the other quantities have both the two uncertainties.

Table 3: Diabatic mechanical efficiency Random and Systematic uncertainties at nominal purge

		Random error				Systematic error			
Parameter	**Nominal**	**Delta**	**Delta [%]**	**Sens**	**D Eff [%]**	**Delta**	**Delta [%]**	**Sens**	**D [%]**
T01	318.555	0.193	0.060%	-1.734	-0.105%	0.350	0.110%	-1.228	-0.135%
Main MF	10.628	0.028	0.265%	-0.991	-0.263%	0.099	0.931%	-0.984	-0.916%
Purge MF	0.054	0.000	0.188%	-0.001	-0.000%	0.001	1.375%	-0.001	-0.002%
Cp main	1003.32	0.938	0.093%	-0.992	-0.093%	-	-	-	-
Cp purge	1002.96	0.242	0.024%	-0.001	-0.000%	-	-	-	-
T0_ini purge	291.454	1.188	0.407%	-0.001	-0.001%	0.350	0.120%	-0.001	-0.000%
P0_ini/P01	0.631	0.004	0.693%	-0.008	-0.005%	0.001	0.224%	-0.008	-0.002%
PDC	0.537	0.002	0.361%	1.474	0.533%	0.001	0.263%	1.472	0.388%
gamma main	1.40027	0.001	0.095%	-2.257	-0.213%	-	-	-	-
gamma purge	1.40047	0.000	0.021%	-0.003	-0.000%	-	-	-	-
Q stator	3740.66	19.33	0.517%	-0.006	-0.003%	452.730	12.103%	-0.006	-0.068%
Q rotor	-22.60	-38.61	170.809%	0.000	0.006%	-55.702	246.426%	0.000	0.009%
Omega	467.439	0.014	0.003%	0.983	0.003%	-	-	-	-
Omega_dot	79.503	0.004	0.005%	0.983	0.005%	-	-	-	-
Inertia	13.496	-	-	-	-	0.061	0.454%	0.983	0.446%
Plosses	8662.56	-	-	-	-	866.26	10.000%	0.017	0.170%
Total					0.647%				1.114%

From Table 3 it is possible to see how the most influencing parameters are the expansion ratio (PDC) and γ of the main flow with a sensitivity of 1.5 and -2.3, respectively. Then, mainstream mass flow rate, rotational speed, acceleration and C_p of the main flow have a sensitivty close to unity (> 0.97).
Finally, random and bias error components obtained for each efficiency definition and for both operating conditions are quite similar: random $\sim$ 0.65% (nominal) and $\sim$ 0.7% (high) and systematic $\sim$ 1.1%.

9. Conclusions

The HSLP turbine stage has been tested in the VKI-CT3 blow-down wind tunnel under two operating conditions. In this kind of facility, the estimation of the efficiency is quite challenging because of the very short time test duration and the non-adiabatic state. In particular, for Mass flow measurements there is not the possibility to install a Venturi or a calibrated orifice. Therefore, a in-house method was used based on a

"zero-dimensional" model of the entire test rig. Due to the operating conditions of the facility, an estimate of the heat transfer through all the stage must be provided. An experimental setup and preliminary results for the rotor inertia measurements, have been also documented. Unfortunately, due to some issues encountered during tests, the efficiency computation has been carried out with an estimate deduced from CAD.
The efficiency calculation is provided with four different definitions. The results show a quite high level of performance. The diabatic indicated efficiency is 0.9233 and 0.9164, respectively, for the nominal and high purge flow conditions. Therefore, a performance drop of 0.7% is experienced for an increase of the purge flow of 100%. Test-to-test repeatability is 0.79% and 0.98% (for nominal and high purge) referred to the indicated efficiency. A significant dispersion of the results related to the thermodynamic efficiency has been found. An uncertainty analysis has been performed, obtaining, for the indicated efficiency, a random error of 0.64% and 0.70% and a systematic error of 1.10% and 1.11% (for nominal and high purge).

References

[1] R. B. Abernethy, R. P. Benedict, and R. B. Dowdell. ASME measurement uncertainty. *Journal of Fluids Engineering*, 107(2):161–164, June 1985.

[2] Nicholas R. Atkins and Roger W. Ainsworth. Turbine aerodynamic performance measurement under nonadiabatic conditions. *Journal of Turbomachinery*, 134(6), August 2012.

[3] Paul F. Beard, Thomas Povey, and Kamaljit S. Chana. Turbine efficiency measurement system for the QinetiQ turbine test facility. *Journal of Turbomachinery*, 132(1), September 2009.

[4] Rémy Denos, Guillermo Paniagua, Tolga Yasa, and Eugenio Forturgno. Determination of the efficiency of a cooled hp turbine in a blow-down facility. 06 2006.

[5] Luca Porreca and Rémy Dénos. Turbine stage mass flow evaluation in a compression tube facility. 2002.

[6] Thomas Povey and Guillermo Paniagua. Method to improve precision of rotating inertia and friction measurements in turbomachinery applications. *Mechanical Systems and Signal Processing*, 30:323–329, July 2012.

[7] T. Yasa. *Efficiency of a high-pressure turbine tested in a compression tube facility*. Doctoral thesis, Université Catholique de Louvain, 2008.